

# Cosmological mass limits on neutrinos, axions, and other light particles

**Steen Hannestad**

Department of Physics, University of Southern Denmark  
Campusvej 55, DK-5230 Odense M, Denmark

**Georg Raffelt**

Max-Planck-Institut für Physik (Werner-Heisenberg-Institut)  
Föhringer Ring 6, 80805 München, Germany

**Abstract.** The small-scale power spectrum of the cosmological matter distribution together with other cosmological data provides a sensitive measure of the hot dark matter fraction, leading to restrictive neutrino mass limits. We extend this argument to generic cases of low-mass thermal relics. We vary the cosmic epoch of thermal decoupling, the radiation content of the universe, and the new particle's spin degrees of freedom. Our treatment covers various scenarios of active plus sterile neutrinos or axion-like particles. For three degenerate massive neutrinos, we reproduce the well-known limit of  $m_\nu < 0.34$  eV. In a 3+1 scenario of 3 massless and 1 fully thermalized sterile neutrino we find  $m_\nu < 1.0$  eV. Thermally produced QCD axions must obey  $m_a < 3.0$  eV, superseding limits from a direct telescope search, but leaving room for solar eV-mass axions to be discovered by the CAST experiment.

## 1. Introduction

The observed universe is surprisingly well described by a simple Friedmann-Robertson-Walker model that is characterized by a handful of well-measured global parameters. Together with the gravitational instability theory for the formation of structure, a “concordance model” has emerged that does not seem to conflict with any firmly established observations. Of course, the physical nature of most of the gravitating matter and energy remains elusive, except that most of the dark matter must be of the cold variety to avoid excessive free streaming in the early universe that would suppress small-scale power of the observed matter distribution. In the framework of this standard paradigm, the observed power spectrum of the cosmic matter distribution provides restrictive limits on the hot dark matter fraction of the cosmological matter cocktail [1].

Taking advantage of the latest cosmological data, notably the 2dF and SDSS galaxy redshift surveys and the WMAP measurement of the cosmic microwave background (CMB) temperature fluctuations, several authors have used this argument to derive restrictive neutrino mass limits of  $\sum m_\nu < 0.7\text{--}1.0$  eV (95% CL) [2–8]. The exact value of the nominal limit depends on the included data sets and on the assumed priors for some of the cosmological parameters. However, the small spread between different nominal limits suggests that the universe is a robust laboratory for constraining the overall neutrino mass scale, and perhaps eventually for positively determining its value [9–12]. Of course, these limits or a future positive detection depend on the validity of the standard cosmological paradigm. For example, the spectrum of primordial density fluctuations may not follow a simple power law, modifying all of these results.

We are here concerned with a different extension of the standard picture in that we study the effect of a non-standard number density of neutrinos, perhaps caused by the existence of additional neutrinos such as sterile states, or new low-mass particles such as axions. One of us has previously shown that increasing the assumed number density of neutrinos actually *weakens* the mass limit, contrary to naive intuition, because the increased radiation density counteracts the effect of the increased hot dark matter fraction [4]. Therefore, the usual neutrino mass limits do not trivially translate into more general cases where the hot dark matter fraction and the radiation content are varied independently.

The free-streaming effect of low-mass particles on the power spectrum of the matter distribution and of the CMB temperature fluctuations depends on the particle mass  $m_X$ , their number density and velocity distribution, and on the radiation content in other degrees of freedom that do not carry mass. We will consider two generic classes of cases. One covers neutrinos, i.e. fermionic degrees of freedom with a momentum distribution given by that of ordinary neutrinos. We vary the mass  $m_\nu$ , the effective number of flavors carrying that mass, and the effective number of massless flavors. Our second generic case is that of particles that were once in thermal equilibrium (thermal relics) so that their contribution to the hot dark matter fraction and their velocity distribution is

perfectly defined by the cosmic temperature  $T_D$  when they thermally decoupled from the background medium, by their mass, and by their number of internal degrees of freedom.

In Sec. 2 we describe our general methodology for deriving the allowed range of non-standard cosmological parameters. In Sec. 3 we apply our method to various scenarios involving active and sterile neutrinos. In Sec. 4 we consider general thermal relics, and finally we conclude in Sec. 5.

## 2. Likelihood Analysis

### 2.1. Theoretical Predictions

In order to derive limits on the parameters characterizing the new particles we compare theoretical power spectra for the matter distribution and the CMB temperature fluctuations with observational data in analogy to the previous works by one of us [3, 4]. The predicted power spectra are calculated with the publicly available CMBFAST package [13]. This package allows one to include directly the effective number of massless neutrino degrees of freedom and of neutrinos carrying a mass as well as the cosmic hot dark matter fraction, assumed to be equally distributed among the massive flavors. Put another way, the standard version of the code assumes a velocity distribution of the neutrinos that ordinary active neutrinos with a mass would have. For our more general case of arbitrary thermal relics we modified the code accordingly.

As a set of cosmological parameters apart from the new particle characteristics we choose the matter density  $\Omega_m$ , the baryon density  $\Omega_b$ , the Hubble parameter  $H_0$ , the scalar spectral index of the primordial fluctuation spectrum  $n_s$ , the optical depth to reionization  $\tau$ , the normalization of the CMB power spectrum  $Q$ , and the bias parameter  $b$ . We restrict our analysis to geometrically flat models  $\Omega = \Omega_m + \Omega_\Lambda = 1$ . Some of the other parameters are not kept entirely free, but are varied over a prior range that is determined from cosmological observations other than CMB and LSS. In flat models the matter density is restricted by observations of Type Ia supernovae to be  $\Omega_m = 0.28 \pm 0.14$  [14]. Furthermore, the HST Hubble key project has obtained a constraint on  $H_0$  of  $72 \pm 8 \text{ km s}^{-1} \text{ Mpc}^{-1}$  [15]. The cosmological parameters and their assumed priors are listed in Table 1. The actual marginalization over parameters was performed using a simulated annealing procedure [16].

### 2.2. Cosmological Data

*2.2.1. Large Scale Structure (LSS).* At present there are two large galaxy surveys of comparable size, the Sloan Digital Sky Survey (SDSS) [17, 18] and the 2dFGRS (2 degree Field Galaxy Redshift Survey) [19]. Once the SDSS is completed in 2005 it will be significantly larger and more accurate than the 2dFGRS. At present the two surveys are, however, comparable in precision and in the present paper we use data from the 2dFGRS alone.

**Table 1.** Priors on cosmological parameters used in the likelihood analysis.

Parameter	Prior	Distribution
$\Omega = \Omega_m + \Omega_\Lambda$	1	Fixed
$\Omega_m$	$0.28 \pm 0.14$	Gaussian
$h$	$0.72 \pm 0.08$	Gaussian
$\Omega_b h^2$	0.014–0.040	Top hat
$n_s$	0.6–1.4	Top hat
$\tau$	0–1	Top hat
$Q$	—	Free
$b$	—	Free

Tegmark, Hamilton and Xu [20] have calculated a power spectrum,  $P(k)$ , from this data, which we use in the present work. The 2dFGRS data extends to very small scales where there are large effects of non-linearity. Since we calculate only linear power spectra, we follow standard procedures and use only data on scales larger than  $k = 0.2 h \text{ Mpc}^{-1}$ , where effects of non-linearity should be minimal (see for instance Ref. [17] for a discussion). With this cut the number of data points for the power spectrum reduces to 18.

*2.2.2. Cosmic Microwave Background.* The temperature fluctuations are conveniently described in terms of the spherical harmonics power spectrum  $C_{T,l} \equiv \langle |a_{lm}|^2 \rangle$ , where  $\frac{\Delta T}{T}(\theta, \phi) = \sum_{lm} a_{lm} Y_{lm}(\theta, \phi)$ . Since Thomson scattering polarizes light, there are also power spectra coming from the polarization. The polarization can be divided into a curl-free ( $E$ ) and a curl ( $B$ ) component, yielding four independent power spectra:  $C_{T,l}$ ,  $C_{E,l}$ ,  $C_{B,l}$ , and the  $T$ - $E$  cross-correlation  $C_{TE,l}$ .

The WMAP experiment has reported data only on  $C_{T,l}$  and  $C_{TE,l}$  as described in Refs. [6, 21–25]. We have performed our likelihood analysis using the prescription given by the WMAP collaboration [6, 21–25] which includes the correlation between different  $C_l$ 's. Foreground contamination has already been subtracted from their published data.

In addition we use other CMB data from the compilation by Wang *et al.* [26] which includes data at higher  $l$ . Altogether this data set has 28 points.

### 3. Neutrinos

#### 3.1. Mass Equally Distributed Among $N_\nu$ Species

Our first class of cases consists of different scenarios with  $N_\nu$  flavors of neutrinos with equal momentum distributions at those early epochs where they are relativistic. Several of these species are assumed to carry equal masses  $m_\nu$ .

The first and simplest example is that of  $N_\nu$  flavors carrying equal masses  $m_\nu$ . In this case the hot-dark matter fraction is given by the standard expression

$$\Omega_\nu h^2 = N_\nu \frac{m_\nu}{91.5 \text{ eV}}, \quad (1)$$

where  $h$  is the Hubble constant in units of  $100 \text{ km s}^{-1} \text{ Mpc}^{-1}$ . Of course, the limiting case  $N_\nu = 3$  corresponds to ordinary neutrinos with a degenerate pattern of masses.

A value for  $N_\nu$  much larger than 3 contradicts the observed primordial helium abundance in the framework of the standard big-bang nucleosynthesis (BBN) theory. However, if the primordial  $\nu_e$  chemical potential takes on a suitable value, its effect on the  $n/p$  freeze-out abundance can always compensate for the expansion-rate effect caused by the additional flavors. Such a fine-tuned  $\nu_e$  degeneracy parameter may not seem particularly plausible, but it serves as one possibility to escape the BBN limits. In any event, we think it is useful to study what can be learned about neutrino parameters from large-scale structure data alone, without combining this information with data pertaining to an entirely different cosmological epoch.

Since we know that the number of ordinary neutrino flavors is exactly 3, the additional degrees of freedom would have to be sterile states, perhaps Dirac partners of the ordinary neutrinos that were thermally equilibrated by some unknown mechanism.

Without sterile states, in principle the effective  $N_\nu$  can be enhanced by suitable neutrino chemical potentials for the ordinary flavors. However, the observed neutrino mixing parameters imply that all three standard flavors reach full thermal equilibrium (i.e. kinetic and chemical equilibrium) before the BBN epoch so that the restrictive BBN limit on the  $\nu_e$  degeneracy parameter applies to all flavors [27]. Therefore, interpreting  $N_\nu > 3$  in terms of an increased density of the ordinary flavors requires some unspecified way to escape the BBN limits. We also note that our treatment assumes a neutrino velocity distribution corresponding to a non-degenerate thermal distribution. Therefore, a case with large neutrino chemical potentials is not strictly covered here.

After marginalizing over the cosmological parameters shown in Table 1, the 68% and 95% CL allowed region of neutrino parameters is shown in Fig. 1. In the left panel this allowed region is shown in the  $N_\nu$ - $\Omega_\nu h^2$ -plane, in the right panel the equivalent region in the  $N_\nu$ - $m_\nu$ -plane.

From the right panel of Fig. 1 it is apparent that the 95% CL upper limit on  $m_\nu$  is nearly independent of  $N_\nu$ , contrary to naive intuition. One of us first observed this effect in Ref. [4]. The limits stated there agree with our present ones that are given explicitly in Table 2 for several values of  $N_\nu$ .

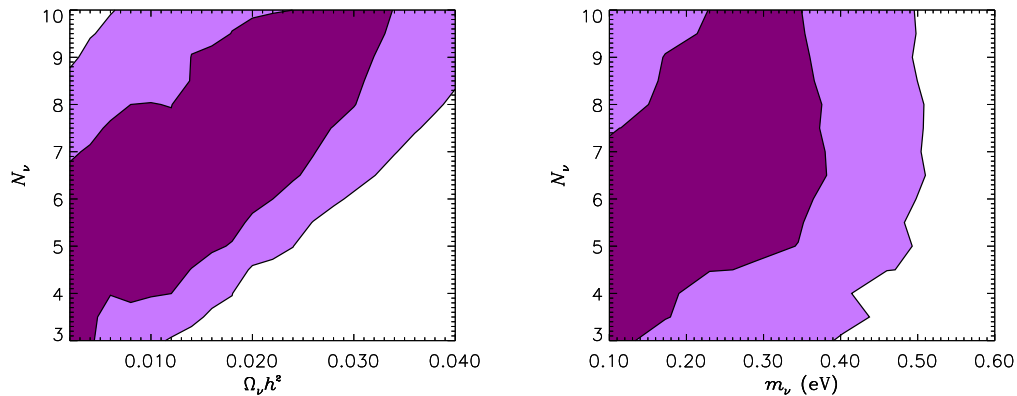


**Figure 1.** Likelihood contours (68% and 95%) for the case of  $N_\nu$  neutrinos with equal masses  $m_\nu$ . Left panel:  $N_\nu$ - $\Omega_\nu h^2$ -plane. Right panel: Equivalent  $N_\nu$ - $m_\nu$ -plane.

**Table 2.** Neutrino mass limits (95% CL) for  $N_\nu$  flavors with equal mass  $m_\nu$ .

Flavors $N_\nu$	Mass limits [eV]	
	$N_\nu m_\nu$	$m_\nu$
3	1.01	0.34
4	1.38	0.35
5	2.12	0.42
6	2.69	0.45

If we specifically assume that the neutrinos are Dirac particles with a degenerate mass spectrum, and that the right-handed partners were thermally equilibrated by some unknown mechanism so that they have equal number densities with the left-handed states, the cosmological mass limit on  $m_\nu$  degrades from 0.34 eV to 0.45 eV.

### 3.2. Mass in One Fully Thermalized Species

As a next case we consider one fully excited neutrino flavor that carries a mass  $m_\nu$  so that the cosmic hot dark matter fraction is given by

$$\Omega_\nu h^2 = \frac{m_\nu}{91.5 \text{ eV}}. \quad (2)$$

In addition there are  $N_\nu - 1$  massless species that contribute to the radiation density. The small mass differences between the ordinary neutrinos imply that this scenario cannot be realized among the ordinary neutrinos so that we need additional sterile states. For example, the 3+1 model for explaining the current neutrino oscillation data including LSND would be a case in point. As in the previous case, one must assume that the BBN limits are circumvented by some mechanism, for example a suitable  $\nu_e$  chemical potential. Since we have 3 flavors of ordinary neutrinos that would contribute to the tally of massless states, and because one fully thermalized species is assumed to carry a mass, the present scenario requires  $N_\nu \geq 4$ . The allowed region of  $N_\nu$ - $m_\nu$ -values is

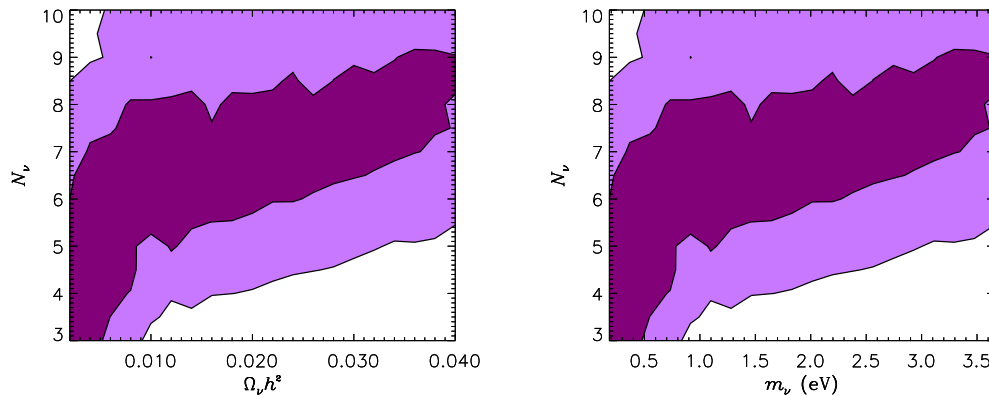


**Figure 2.** Likelihood contours (68% and 95%) for the case of  $N_\nu$  flavors with one of them carrying a mass  $m_\nu$ . Left panel:  $N_\nu$ - $\Omega_\nu h^2$ -plane. Right panel: Equivalent  $N_\nu$ - $m_\nu$ -plane.

**Table 3.** Neutrino mass limits (95% CL) for  $N_\nu$  flavors with exactly one of them carrying mass  $m_\nu$ .

Flavors	Mass limit [eV]
3	0.73
4	1.05
5	2.47
6	4.13

shown in Fig. 2 where we have extended the plot down to  $N_\nu = 3$ . In Table 3 we give explicit numerical 95% CL mass limits for several values of  $N_\nu$ .

### 3.3. Three “Massless” Standard Neutrinos

Our last neutrino example is one where we consider the three standard neutrinos to have very small hierarchical masses, i.e. to be effectively massless for our purpose. In addition we assume there to be  $N_\nu - 3$  other flavors, e.g. sterile states, that carry equal masses  $m_\nu$  so that the hot dark matter fraction is

$$\Omega_\nu h^2 = (N_\nu - 3) \frac{m_\nu}{91.5 \text{ eV}}. \quad (3)$$

An example would be a scenario with an additional sterile neutrino that did not reach full thermal equilibrium so that it is present with less than one full effective degree of freedom.

The allowed region of  $N_\nu$ - $m_\nu$ -values is shown in Fig. 3. In Table 4 we give explicit numerical 95% CL mass limits for several values of  $N_\nu$ . Note that the case  $N_\nu = 4$  is identical to the  $N_\nu = 4$  case in the preceding section. The slight difference in quoted mass limit (1.02 eV instead of 1.05 eV) is due to the fact that the limit is interpolated from the calculated likelihood grid.

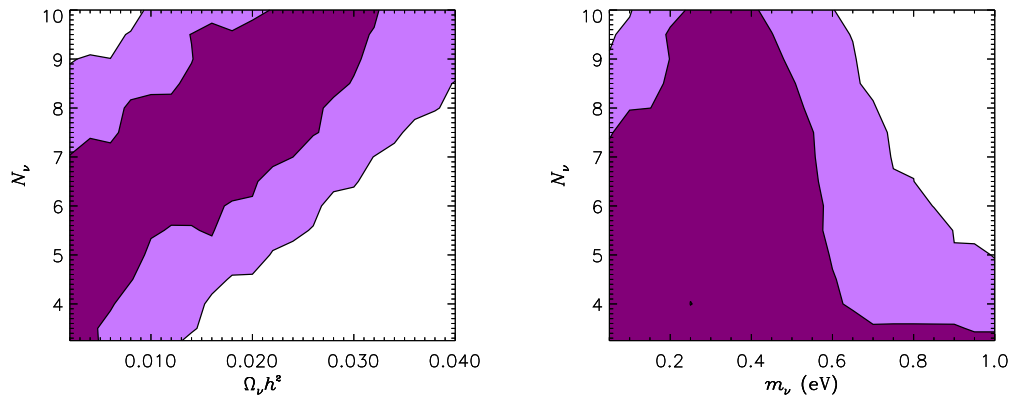


**Figure 3.** Likelihood contours (68% and 95%) for the case of  $N_\nu$  flavors,  $N_\nu - 3$  each carrying mass  $m_\nu$ , and an additional 3 massless flavors.

**Table 4.** Neutrino mass limits for the case of  $N_\nu$  species, with 3 massless flavors and  $N_\nu - 3$  massive neutrinos, each carrying mass  $m_\nu$ .

Flavors	Mass limit [eV]
3.25	2.95
3.50	1.67
3.75	1.21
4.00	1.02
4.50	0.87
5.00	0.82
5.50	0.77
6.00	0.71

Note that for less than one massive species the mass limit becomes quite poor because the limit on  $\Omega_\nu h^2$  remains almost constant down to  $N_\nu = 3.25$ , whereas the limit on  $m_\nu$  is proportional to  $1/(N_\nu - 3)$ .



## 4. General Thermal Relics

### 4.1. Low-Mass Fermions

Our second generic class of models is that of some new particle with mass  $m_X$  that was once in thermal equilibrium, but decoupled when the universe had a temperature  $T_D$  and the radiation density was characterized by  $g_{*D}$  effective thermal degrees of freedom. The relevant masses are of order eV so that the particles decouple when they are relativistic, i.e. at decoupling they are characterized by a Fermi-Dirac or Bose-Einstein distribution of temperature  $T_D$ .

In the present-day universe, the new particles will be non-relativistic and contribute a matter fraction

$$\Omega_X h^2 = \frac{m_X g_X}{183 \text{ eV}} \frac{g_{*\nu}}{g_{*D}} \times \begin{cases} 1 & \text{fermions} \\ \frac{4}{3} & \text{bosons} \end{cases} \quad (4)$$

where  $g_X$  is the number of the particle's internal degrees of freedom while  $g_{*\nu}$  is the effective number of thermal degrees of freedom when ordinary neutrinos freeze out with  $g_{*\nu} = 10.75$  in the absence of new particles. For the case of  $N_\nu$  ordinary neutrinos with equal masses (degenerate mass scenario) we have  $g_X = 2N_\nu$  (two spin degrees for each flavors),  $T_D \approx 2 \text{ MeV}$  and thus  $g_{*D} = g_{*\nu}$  so that Eq. (4) corresponds to the usual result  $\Omega_\nu h^2 = N_\nu m_\nu / 91.5 \text{ eV}$  as stated already in Eq. (1).

In the late epochs that are important for structure formation, the momentum distribution of the new particles is characterized by a thermal distribution with temperature  $T_X$  that is given by

$$\frac{T_X}{T_\nu} = \left( \frac{g_{*D}}{g_{*\nu}} \right)^{1/3}. \quad (5)$$

We have modified CMBFAST to incorporate a fermionic thermal relic with such a momentum distribution.

Our first case is  $g_X = 2$ , i.e. a Majorana fermion with interactions that can be weaker than those of ordinary neutrinos. The limits are calculated with a Fermi-Dirac distribution, but they would not change significantly for the Bose-Einstein case. In Fig. 4 we show the 68% and 95% likelihood contours for the allowed parameters in terms of  $\Omega_X h^2$  and  $T_X/T_\nu$ . Limits for selected values of  $T_X/T_\nu$  can be found in Table 5. Of course, in the limit  $T_X/T_\nu = 1$  we recover the 3+1 scenario of 3 ordinary massless neutrinos and one extra flavor with mass  $m_\nu$ .

Figure 4 reveals that the bound on  $\Omega_X h^2$  is almost independent of  $T_X$  down to a critical value. For lower  $T_X$  the bound abruptly relaxes, allowing for a large mass fraction  $\Omega_X$  of the new particles. This behavior is explained by our non-linearity cut in the data at  $k = 0.2 h \text{ Mpc}^{-1}$ . For low values of  $T_X$  the free-streaming scale of the particles is simply too small to affect large-scale structures above the cut.

In order to substantiate this interpretation we note that the free-streaming scale

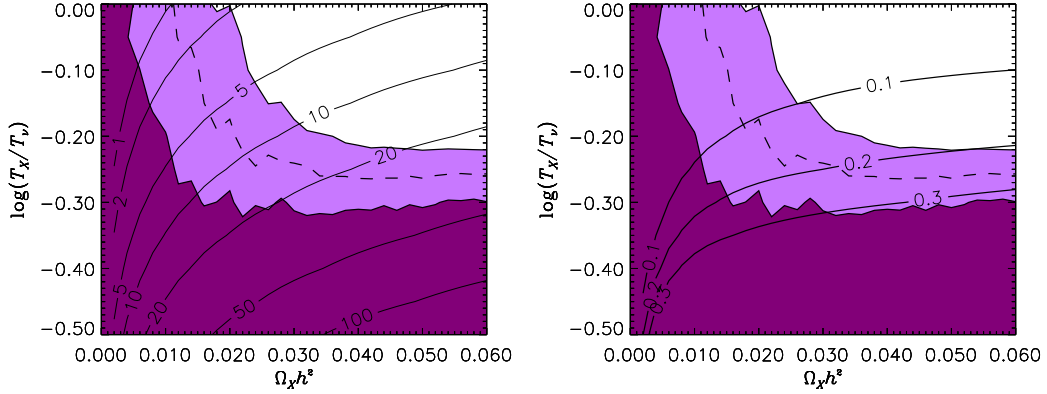


**Figure 4.** Likelihood contours (68% and 95%) for a generic thermal relic with  $g_X = 2$ , characterized by its density,  $\Omega_X h^2$ , and effective temperature,  $T_X$ . The dashed line shows  $\Delta\chi^2 = 4$ , corresponding to the 95% confidence limit for *fixed*  $T_X$ . In the left panel, the solid lines correspond to the indicated values of the particle mass in eV, whereas in the right panel they denote the parameters for which the free streaming scale according to Eq. (6) is  $k_{\text{FS}} = 0.1, 0.2$ , and  $0.3 h \text{ Mpc}^{-1}$ .

**Table 5.** Limits (95% CL) for  $g_X = 2$ , i.e. a general Majorana fermion.

$\log(T_X/T_\nu)$	$T_X/T_\nu$	$g_{*D}/g_{*\nu}$	Upper limit	
			$\Omega_X h^2$	$m_X$ [eV]
0.00	1.000	1.00	0.011	1.0
-0.05	0.891	1.41	0.012	1.6
-0.10	0.794	2.00	0.015	3.0
-0.15	0.708	2.82	0.017	4.1
-0.20	0.631	3.98	0.021	7.5
-0.25	0.562	5.62	0.029	15.0
-0.30	0.501	7.94	No bounds.	

can be approximated as

$$\lambda_{\text{FS}} = \frac{2\pi}{k_{\text{FS}}} \sim \frac{20 \text{ Mpc}}{\Omega_X h^2} \left(\frac{T_X}{T_\nu}\right)^4 \left\{ 1 + \log \left[ 3.9 \frac{\Omega_X}{\Omega_m} \left(\frac{T_\nu}{T_X}\right)^2 \right] \right\}. \quad (6)$$

In the right panel of Fig. 4 we show contours for which  $k_{\text{FS}} = 0.1, 0.2$ , and  $0.3 h \text{ Mpc}^{-1}$ . Evidently  $k_{\text{FS}} = 0.2 h \text{ Mpc}^{-1}$  corresponds fairly well to the value of  $T_X$  where the constraint on  $\Omega_X h^2$  disappears. An exact match can not be expected because our estimate was only approximate. Moreover, the  $X$ -particles follow a thermal distribution so that some fraction will have large energies and therefore stream further than the mean of the distribution. Therefore, there is some free-streaming effect above our cut even if the mean free streaming scale is too small.

We note that even though the galaxy data from surveys such as 2dFGRS or SDSS must be cut at  $0.2 h \text{ Mpc}^{-1}$ , data from the Lyman- $\alpha$  forest measure an earlier cosmological epoch and thus the linear regime extends to much larger values of  $k$ .

For instance, this was used in Ref. [28] to constrain the possible mass of a thermally produced warm dark matter particle to be  $m_X \gtrsim 750$  eV, assuming that it provides all the dark matter. In our paper we have deliberately avoided the Lyman- $\alpha$  data since the conversion of the measured flux power spectrum into a matter power spectrum is fraught with difficulties and the result is at present highly controversial.

For a particle freezing out after the QCD phase transition, the effective number of thermal degrees of freedom at decoupling is  $g_{*D} \lesssim 20$  or  $g_{*D}/g_{*\nu} \lesssim 2$  so that the mass bounds are quite restrictive,  $m_X < 3$  eV or better. However, at the QCD phase transition,  $g_*$  decreases dramatically due to the large number of confined colored degrees of freedom. At epochs shortly before the transition  $g_* \gtrsim 60$  so that a particle freezing out at that time is characterized by  $g_{*D}/g_{*\nu} \gtrsim 6$ , preventing us from stating any significant bounds without using the Lyman- $\alpha$  data.

#### 4.2. Scalar Bosons

The cosmic mass fraction of our new particles is proportional to  $g_X m_X$  so that the limits of the previous section can be roughly scaled to cases with a different number of internal degrees of freedom  $g_X$ . Also, on the basis of the estimated free-streaming scale one can estimate for which value of  $T_X/T_\nu$  the mass limits begin to fail. Still, we have performed an explicit analysis for another special case, the one of a scalar or pseudoscalar boson ( $g_X = 1$ ). This example is of particular interest for axions or axion-like particles.

The results of our likelihood analysis are shown in Fig. 5, which is fully analogous to Fig. 4. We also tabulate explicit  $m_X$  limits for selected values of  $T_X/T_\nu$  in Table 6. We note that for particles decoupling after the QCD phase transition the mass limit for equivalent decoupling epochs is only slightly weaker than it is for the previous  $g_X = 2$  case, i.e. the simple  $m_X \propto g_X^{-1}$  scaling would have yielded less restrictive limits. The free-streaming scale enters the non-linear regime at higher  $T_X$  than before. Once more we find that there is no meaningful mass limit for particles decoupling before the QCD epoch.

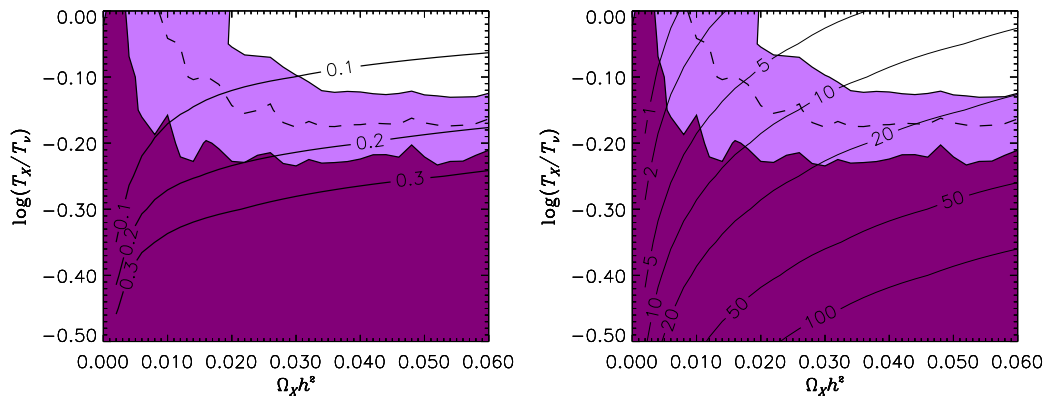


**Figure 5.** Same as Fig. 4 for scalar bosons ( $g_X = 1$ ).

**Table 6.** Limits (95% CL) for  $g_X = 1$ , i.e. a general scalar or pseudoscalar boson.

$\log(T_X/T_\nu)$	$T_X/T_\nu$	$g_{*D}/g_{*\nu}$	Upper limit	
			$\Omega_X h^2$	$m_X$ [eV]
0.00	1.000	1.00	0.009	1.2
-0.05	0.891	1.41	0.011	2.0
-0.10	0.794	2.00	0.013	3.3
-0.15	0.708	2.82	0.020	7.8
-0.20	0.631	3.98	No bounds.	

As a concrete example we mention axions. The energy-loss limit from SN 1987A implies that the axion mass is bounded by  $m_a \lesssim 10^{-2}$  eV [29]. Therefore, it is usually assumed that cosmologically significant axions must be non-thermal relics with very small masses. On the other hand, the SN 1987A argument may have loop holes or one may assume that the axion couplings, notably those to photons, are quite different from the most common models, perhaps allowing eV-mass axions to exist in the “hadronic axion window” [30]. If the axion mass is in the eV range, its couplings to nucleons and pions is so strong that it decouples thermally well after the QCD transition [31, 32]. According to Table 6 this implies a cosmological mass limit of  $m_a < 2\text{--}3$  eV.

In a direct telescope search, narrow lines from the two-photon decay of axions trapped in galaxy clusters were searched in the mass range 3–8 eV [33], but no signal was found. According to our new limits, axions in this mass range can not exist because of their excessive free-streaming effect on cosmic structures.

On the other hand, the possibility of axion-like particles that couple only to photons by virtue of their  $\pi^0$ -like two-photon vertex is sometimes discussed [34, 35]. For an interaction strength small enough to obey the well-known globular-cluster limit [29], such particles would decouple well before the QCD epoch [34]. Therefore, our arguments do not provide any new limits on such hypothetical particles.

Either way, our limits do not infringe on the possibility that the CAST experiment at CERN to search for solar axions could discover axions or axion-like particles with masses up to the eV range [36]. Actually, a small gap will remain between our new limits and CAST’s future high-mass frontier.

## 5. Discussion and Summary

We have calculated general cosmological bounds on the masses and abundances of light, stable particles such as neutrinos and axions. For neutrinos we have calculated three different generic cases:

- 1) All neutrinos are massive, so that there are  $N_\nu$  neutrinos, each with mass  $m_\nu$ .
- 2) Only one neutrino is massive, but altogether there are  $N_\nu$  neutrinos.
- 3) There are three massless neutrinos and  $N_\nu - 3$  species with mass  $m_\nu$ .

In each case it is found that there is a strong correlation between  $\Omega_\nu h^2$  and  $N_\nu$ , but not necessarily between  $m_\nu$  and  $N_\nu$ .

We have extended the standard analysis to include generic light particles such as axions and majorons. We assume such particles to have been thermally produced so that they are characterized by an effective temperature  $T_X$ . The other free parameter can be taken to be either  $\Omega_X h^2$  or  $m_X$ , but since  $\Omega_X h^2$  is the main parameter entering into CMB and LSS calculations we chose the parameters to be  $\Omega_X h^2$  and  $T_X$ .

In our analysis we do not use LSS data in the non-linear regime, i.e. at small scales, and we also do not use Lyman- $\alpha$  data. Therefore, particles that decouple too early and thus today have much smaller momenta than neutrinos do not produce significant free-streaming effects on the relevant scales. It turns out that for both spin- $\frac{1}{2}$  fermions and for scalars that decouple before the QCD epoch, we can not state a significant mass limit. On the other hand, for such particles decoupling after the QCD epoch, there is a mass limit between 1–3 eV, depending on the spin and exact epoch of decoupling. For the case of axions, our limits supersede previous results from direct telescope searches for axion decays.

## Acknowledgments

We acknowledge use of the publicly available CMBFAST package [13] and of computing resources at DCSC (Danish Center for Scientific Computing). We acknowledge support by the European Science Foundation (ESF) under the Network Grant No. 86 Neutrino Astrophysics. In Munich, this work was supported, in part, by the Deutsche Forschungsgemeinschaft (DFG) under grant No. SFB-375.

## References

- [1] W. Hu, D. J. Eisenstein and M. Tegmark, “Weighing neutrinos with galaxy surveys,” *Phys. Rev. Lett.* **80** (1998) 5255 [astro-ph/9712057].
- [2] O. Elgaroy *et al.*, “A new limit on the total neutrino mass from the 2dF galaxy redshift survey,” *Phys. Rev. Lett.* **89**, 061301 (2002) [astro-ph/0204152].
- [3] S. Hannestad, “Cosmological limit on the neutrino mass,” *Phys. Rev. D* **66** (2002) 125011 [astro-ph/0205223].
- [4] S. Hannestad, “Neutrino masses and the number of neutrino species from WMAP and 2dFGRS,” *JCAP* **0305** (2003) 004 [astro-ph/0303076].
- [5] O. Elgaroy and O. Lahav, “The role of priors in deriving upper limits on neutrino masses from the 2dFGRS and WMAP,” *JCAP* **0304** (2003) 004 [astro-ph/0303089].
- [6] D. N. Spergel *et al.*, “First year Wilkinson Microwave Anisotropy Probe (WMAP) observations: Determination of cosmological parameters,” *Astrophys. J. Suppl.* **148** (2003) 175 [astro-ph/0302209].
- [7] S. W. Allen, R. W. Schmidt and S. L. Bridle, “A preference for a non-zero neutrino mass from cosmological data,” astro-ph/0306386.
- [8] V. Barger, D. Marfatia and A. Tregre, “Neutrino mass limits from SDSS, 2dFGRS and WMAP,” hep-ph/0312065.

- [9] S. Hannestad, “Can cosmology detect hierarchical neutrino masses?,” *Phys. Rev. D* **67** (2003) 085017 [astro-ph/0211106].
- [10] K. N. Abazajian and S. Dodelson, “Neutrino mass and dark energy from weak lensing,” *Phys. Rev. Lett.* **91** (2003) 041301 [astro-ph/0212216].
- [11] M. Kaplinghat, L. Knox and Y. S. Song, “Determining neutrino mass from the CMB alone,” [astro-ph/0303344].
- [12] S. Bashinsky and U. Seljak, “Neutrino perturbations in CMB anisotropy and matter clustering,” [astro-ph/0310198].
- [13] U. Seljak and M. Zaldarriaga, “A line of sight approach to cosmic microwave background anisotropies,” *Astrophys. J.* **469** (1996) 437 [astro-ph/9603033]. See also the CMBFAST website at <http://cosmo.nyu.edu/matiasz/CMBFAST/cmbfast.html>
- [14] S. Perlmutter *et al.* [Supernova Cosmology Project Collaboration], “Measurements of Omega and Lambda from 42 high-redshift supernovae,” *Astrophys. J.* **517** (1999) 565 [astro-ph/9812133].
- [15] W. L. Freedman *et al.*, “Final results from the Hubble Space Telescope key project to measure the Hubble constant,” *Astrophys. J.* **553** (2001) 47 [astro-ph/0012376].
- [16] S. Hannestad, “Stochastic optimization methods for extracting cosmological parameters from cosmic microwave background radiation power spectra,” *Phys. Rev. D* **61** (2000) 023002.
- [17] M. Tegmark *et al.* [SDSS Collaboration], “Cosmological parameters from SDSS and WMAP,” astro-ph/0310723.
- [18] M. Tegmark *et al.* [SDSS Collaboration], “The 3D power spectrum of galaxies from the SDSS,” astro-ph/0310725.
- [19] M. Colless *et al.*, “The 2dF Galaxy Redshift Survey: Final data release,” astro-ph/0306581.
- [20] M. Tegmark, A. J. S. Hamilton and Y. Xu, “The power spectrum of galaxies in the 2dF 100k redshift survey,” *Mon. Not. Roy. Astron. Soc.* **335**, 887 (2002) [astro-ph/0111575].
- [21] C. L. Bennett *et al.*, “First year Wilkinson Microwave Anisotropy Probe (WMAP) observations: Preliminary maps and basic results,” *Astrophys. J. Suppl.* **148** (2003) 1 [astro-ph/0302207].
- [22] A. Kogut *et al.*, “Wilkinson Microwave Anisotropy Probe (WMAP) first year observations: TE polarization,” *Astrophys. J. Suppl.* **148** (2003) 161 [astro-ph/0302213].
- [23] G. Hinshaw *et al.*, “First year Wilkinson Microwave Anisotropy Probe (WMAP) observations: Angular power spectrum,” *Astrophys. J. Suppl.* **148** (2003) 135 [astro-ph/0302217].
- [24] L. Verde *et al.*, “First year Wilkinson Microwave Anisotropy Probe (WMAP) observations: Parameter estimation methodology,” *Astrophys. J. Suppl.* **148** (2003) 195 [astro-ph/0302218].
- [25] H. V. Peiris *et al.*, “First year Wilkinson Microwave Anisotropy Probe (WMAP) observations: Implications for inflation,” *Astrophys. J. Suppl.* **148** (2003) 213 [astro-ph/0302225].
- [26] X. Wang, M. Tegmark, B. Jain and M. Zaldarriaga, “The last stand before MAP: Cosmological parameters from lensing, CMB and galaxy clustering,” astro-ph/0212417.
- [27] A. D. Dolgov, S. H. Hansen, S. Pastor, S. T. Petcov, G. G. Raffelt and D. V. Semikoz, “Cosmological bounds on neutrino degeneracy improved by flavor oscillations,” *Nucl. Phys. B* **632** (2002) 363 [hep-ph/0201287].
- [28] V. K. Narayanan, D. N. Spergel, R. Dave and C. P. Ma, “Lyman-alpha forest constraints on the mass of warm dark matter and the shape of the linear power spectrum,” *Astrophys. J. Lett.* **543** (2000) L103 [astro-ph/0005095].
- [29] G. G. Raffelt, “Particle physics from stars,” *Ann. Rev. Nucl. Part. Sci.* **49** (1999) 163 [hep-ph/9903472].
- [30] T. Moroi and H. Murayama, “Axionic hot dark matter in the hadronic axion window,” *Phys. Lett. B* **440** (1998) 69 [hep-ph/9804291].
- [31] M. S. Turner, “Thermal production of not so invisible axions in the early universe,” *Phys. Rev. Lett.* **59** (1987) 2489 [Erratum-*ibid.* **60** (1988) 1101].
- [32] S. Chang and K. Choi, “Hadronic axion window and the big bang nucleosynthesis,” *Phys. Lett. B* **316** (1993) 51 [hep-ph/9306216].
- [33] M. A. Bershadsky, M. T. Ressel and M. S. Turner, “Telescope search for multi-eV axions,” *Phys.*

- Rev. Lett. **66** (1991) 1398.
- [34] E. Massó and R. Toldrà, “On a light spinless particle coupled to photons,” Phys. Rev. D **52** (1995) 1755 [hep-ph/9503293].
- [35] E. Massó and R. Toldrà, “New constraints on a light spinless particle coupled to photons,” Phys. Rev. D **55** (1997) 7967 [hep-ph/9702275].
- [36] J. I. Collar *et al.* [CAST Collaboration], “CAST: A search for solar axions at CERN,” hep-ex/0304024.